

**Weierstraß-Institut**  
**für Angewandte Analysis und Stochastik**  
**Leibniz-Institut im Forschungsverbund Berlin e. V.**

Preprint

ISSN 2198-5855

**Fractal homogenization of a multiscale interface problem**

Martin Heida<sup>1</sup>, Ralf Kornhuber<sup>2</sup>, Joscha Podlesny<sup>2</sup>

submitted: December 4, 2017

<sup>1</sup> Weierstraß-Institut  
Mohrenstr. 39  
10117 Berlin  
Germany  
E-Mail: martin.heida@wias-berlin.de

<sup>2</sup> Institut für Mathematik  
Freie Universität Berlin  
14195 Berlin  
Germany  
E-Mail: kornhuber@math.fu-berlin.de  
podlesjo@math.fu-berlin.de

No. 2453  
Berlin 2017



---

2010 *Mathematics Subject Classification.* 74B05, 74Qxx, 74Q05, 65M22, 65M55.

*Key words and phrases.* Multiscale interfaces, fractal homogenization, elasticity, jump conditions, multiscale numerics.

This research has been funded by Deutsche Forschungsgemeinschaft (DFG) through grant CRC 1114 "Scaling Cascades in Complex Systems", Project C05 "Effective models for interfaces with many scales" and Project B01 "Fault networks and scaling properties of deformation accumulation".

Edited by  
Weierstraß-Institut für Angewandte Analysis und Stochastik (WIAS)  
Leibniz-Institut im Forschungsverbund Berlin e. V.  
Mohrenstraße 39  
10117 Berlin  
Germany

Fax: +49 30 20372-303  
E-Mail: [preprint@wias-berlin.de](mailto:preprint@wias-berlin.de)  
World Wide Web: <http://www.wias-berlin.de/>

# Fractal homogenization of a multiscale interface problem

Martin Heida, Ralf Kornhuber, Joscha Podlesny

## Abstract

Inspired from geological problems, we introduce a new geometrical setting for homogenization of a well known and well studied problem of an elliptic second order differential operator with jump condition on a multiscale network of interfaces. The geometrical setting is fractal and hence neither periodic nor stochastic methods can be applied to the study of such kind of multiscale interface problem. Instead, we use the fractal nature of the geometric structure to introduce smoothed problems and apply methods from a posteriori theory to derive an estimate for the order of convergence. Computational experiments utilizing an iterative homogenization approach illustrate that the theoretically derived order of convergence of the approximate problems is close to optimal.

## 1 Introduction

The classical elliptic homogenization problem considers a second order differential equation

$$-\nabla (A^\varepsilon \nabla u_\varepsilon) = f,$$

where  $A^\varepsilon(x) = A\left(\frac{x}{\varepsilon}\right)$  for a coefficient field  $A$ . Hence, the oscillations of the microscopic structure  $A^\varepsilon$  usually is of size  $\varepsilon$  compared to the diameter of the macroscopic domain. For example, in periodic homogenization, the coefficient  $A$  is  $Y$ -periodic, where  $Y = [0, 1]^d$  is the unit cell in  $\mathbb{R}^d$ . In stochastic homogenization, the random geometry  $A^\varepsilon(x)$  is described by a random variable on a probability space  $A: \Omega \rightarrow \mathbb{R}$  and a dynamical system  $(\tau_x)_{x \in \mathbb{R}^d}$  on  $\Omega$  such that a formula of the type  $A^\varepsilon(x) = A(\tau_{\frac{x}{\varepsilon}} \omega)$  holds. There have been developed lots of tools for qualitative homogenization results, and we refer to [1, 2, 5, 11] for the periodic case and to [14, 24] for the stochastic case. For quantitative results, we refer to [3, 4, 5, 8, 9].

In models for polycrystals or composite materials, the elliptic equation in the bulk is complemented by a jump condition on a microscopic interface  $\Gamma^\varepsilon$ . For example, in the periodic setting we could consider a piecewise smooth  $Y$ -periodic hypermanifold  $\Gamma$  with  $\Gamma^\varepsilon := \varepsilon\Gamma$ . On  $\Gamma^\varepsilon$  we make a unique choice of a normal field  $\nu$ , denote by  $\llbracket u_\varepsilon \rrbracket_\nu$  the jump of  $u_\varepsilon$  in direction  $\nu$  and impose the condition

$$-\partial_\nu u_\varepsilon = \llbracket u_\varepsilon \rrbracket_\nu \quad \text{on } \Gamma^\varepsilon.$$

The corresponding stochastic construction can be found in [10, 13]. The homogenization of such problems with a scaling parameter  $\varepsilon$  has been studied in great detail with many generalizations, starting from the work in [12, 13]. In this setting, the size of the grains

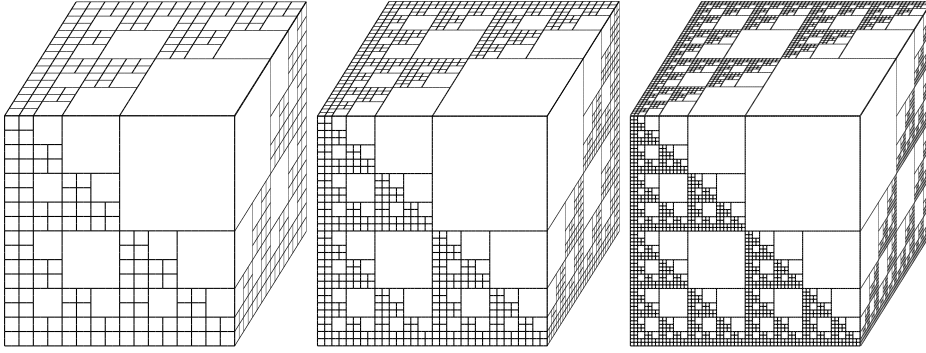


Figure 1: Level interface networks  $\Gamma^{(K)}$  for  $K = 4, 5$  and  $6$ . Evidently, the geometry is multiscale but not suited for periodic or stochastic homogenization.

is always of order  $\varepsilon$  compared to the macroscopic domain. In particular, they are of approximately the same size.

In the above context, stochastic and periodic homogenization problems usually imply a priori the assumption of separation of scales: It is assumed that there exists a scaling parameter  $\varepsilon$  who captures the rate of oscillations in the coefficients: all relevant scales are given as positive powers of  $\varepsilon$ . Thus, in the analytical limit  $\varepsilon \rightarrow 0$ , usually the problems decouple into one macroscopic problem that describes the macroscopically observed behavior of the system, and one or several (depending on the amount of scales) microscopic problems (known as *cell-problems*).

In this work, we study the above analytic problem in a non-standard geometric setting motivated by geology. It is known that in nature the size of the grains in fractured rock is distributed in a fractal sense. In particular, this means that the size of grains and of interfaces are distributed according to an exponential law. Experimental studies show that the cumulative number  $N(r)$  of fragments whose size is bigger than  $r$  scales according to

$$N(r) = Cr^{-D}. \quad (1)$$

$D$  is often called the fractal dimension. In order to understand this distribution, Sammis et al [20] have proposed a model of fragmentation in tectonic deformation which is based on the assumption that the interaction of two neighbored blocks of equal size under deformation will lead to breakeage of one of these blocks. In their model, it is unlikely, that a bigger block breaks a smaller block or vice versa. Mathematically, this results in a Cantor-type geometry. For further reading, refer to [19, 21]. In the present studies, we do not explicitly require an exponential law of grainsize distribution but focus on a slightly more general setting.

Hence, a particular feature of our geometrical model is the non-separability of the inherent scales, that is: We cannot a priori identify a scale parameter  $\varepsilon$  mathematically separating a *physically small* scale from a *physically large* scale. In particular, we are interested in a case such as depicted in Figure 1, where the size distribution of cells does not allow for any scale separation, i.e. where the size of cells ranges from *arbitrarily small* to *half of the domain*  $Q$  and the scales are separated by a factor  $\frac{1}{2}$ . For completeness, we mention that the resulting geometry does also not satisfy ergodicity or stationarity, necessary assumptions in stochastic homogenization.

As explained above, classical homogenization techniques are not suited to address this multiscale interface problem. Our analytical ansatz is the following: We use the hierar-

chical self-similar structure of  $\Gamma$  in order to provide a sequence of interfaces  $\Gamma^{(K)}$  (see Fig. 1) that “converge” to  $\Gamma$  as  $K \rightarrow \infty$ . For each  $K$ , we solve the corresponding problem denoting the solution as  $u_K$ , and ask how much the solution  $u_K$  changes between the steps  $K$  and  $K+L$ . In Theorem 2.6 we show, that for fixed  $K$  the distance  $\|u_K - u_{K+L}\| = o(e^{-CK})$  is uniformly bounded for all  $L$  and decreases exponentially to 0 for  $K \rightarrow \infty$ .

In summary, the key observations from our analytical investigation are the following. Although our multiscale interface problem is a homogenization problem in the true original meaning of the word, it seems that classical stochastic and periodic homogenization techniques are not helpful for fractal structures that lack scale separation. Alternatively, in case that the ever finer geometrical structure concentrates on a subset of small Lebesgue-measure, we might locally replace the fractal structure by a smoothed one such that the total error between the solutions of the exact and the smoothed problem are small. However, we believe that this type of multiscale interface problems open an interesting new area within the family of homogenization problems, which we refer to as *fractal homogenization*.

Interestingly, the numerical study of the elliptic problems with oscillating coefficients leads to similar difficulties and the way to overcome them is in some sense related to the analytical approach. For computational purposes, a global discretization of all scales is unfeasible. Thus, the multiscale problem is often decomposed into a global problem associated with an intentionally coarse finite element grid and local auxiliary subproblems. The specific setup of global and local problems characterizes the individual methods. Well-established approaches to such kind of numerical homogenization mimic analytical paradigms and thus suffer from corresponding restrictions on scale separation or periodicity [6]. One notable exception is the contribution by Målqvist and Peterseim [18] that relies on localized orthogonal subspace decomposition (LOD). In order to establish a low dimensional multiscale basis, coarse basis functions are enriched with corrections from localized, decoupled fine scale problems. This leads to quasioptimal energy and  $L^2$  error estimates without any additional assumptions on periodicity or scale separation. A related method derived and analyzed in the general framework of subspace correction is featuring suitable smoothers for localization and exhibits the same generality in the assumptions on the oscillating coefficients [15]. While these methods aim at a kind of model reduction, iterative numerical homogenisation methods [16, 17] are designed for solving the given multiscale problem up to a certain accuracy.

In this paper, we apply iterative numerical homogenization [16, 17] to multiscale interface problems as described above. From a physical point of view, any computational implementation of partial differential equations on fractal geometries such as depicted in Figure 1 should resolve the interface  $\Gamma$  and the jumps of  $u$  on the macroscopically relevant scales. Also from a physical point of view, we expect that small structures have only minor effects on the macroscopic behavior. This motivates to successively resolve the fractal geometry by an sequence of meshes  $\mathcal{T}_0, \dots, \mathcal{T}_K$  and to compute approximations  $\tilde{u}_K$  of  $u_K$ . To this end, we introduce a decomposition of the corresponding finite element space  $S^{(K)}$  into a coarse space and a hierarchy of local spaces associated with a spatial hierarchy of local patches that successively resolve the interfaces  $\Gamma^{(0)}, \dots, \Gamma^{(K)}$ . This decomposition induces an additive Schwarz preconditioner that accelerates the convergence of a global conjugate gradient iteration. We first illustrate the analytically predicted behavior of (approximations  $\tilde{u}_K$  of)  $u_K$  numerically. In further numerical experiments with a Cantor-type geometry and a typical geological fault network, we observe that the convergence rates

of our iterative scheme appears to be robust with respect to increasing  $K$ . Theoretical justification and extensions to model reduction in the spirit of [15, 18] will be carried out in a separate publication.

The paper is structured as follows. In Section 2 we will introduce a precise formulation of multiscale interface problems and formulate our main results on fractal homogenization. In Section 3 we provide suitable local and global Poincaré inequalities to prepare the proofs of our main results as carried out in Section 4. Section 5 is devoted to numerical experiments illustrating the theoretical findings and the efficiency and reliability of iterative numerical homogenization.

## 2 Main results

### 2.1 Geometric setting

Let  $\mathcal{Q}$  be a bounded domain in  $\mathbb{R}^d$  and let  $\Gamma = \bigcup_{k \in \mathbb{N}} \Gamma_k$ , where each  $\Gamma_k$  is of finite  $(n-1)$ -dimensional Hausdorff measure, i.e.  $\mathcal{H}^{d-1}(\Gamma_k) < \infty$  and  $\Gamma_k$  is locally affine except for a set of zero  $(d-1)$ -dimensional Hausdorff measure. Define the level interface networks  $\Gamma^{(K)} := \bigcup_{k=1}^K \Gamma_k$ . For every  $K \in \mathbb{N}$  the domain  $\mathcal{Q} \setminus \Gamma^{(K)}$  splits into cells  $(G_i^{(K)})_{i=1, \dots, I_K}$ , i.e.

$$\mathcal{Q} \setminus \Gamma^{(K)} = \bigcup_{i=1, \dots, I_K} G_i^{(K)},$$

where each  $G_i^{(K)}$  is open, simply connected with  $\partial G_i^{(K)} = \overline{\partial G_i^{(K)}}$ . We denote  $\mathcal{G}^{(K)} := \{G_i^{(K)} : i = 1, \dots, I_K\}$  and

$$\begin{aligned} \mathcal{G}_\infty^{(K)} &:= \{G \in \mathcal{G}^{(K)} : \forall L > K \text{ holds } G \in \mathcal{G}^{(L)}\}, \\ d_K &:= \max \left\{ \text{diam } G : G \in \mathcal{G}^{(K)} \setminus \mathcal{G}_\infty^{(K-1)} \right\}, \end{aligned}$$

where we assume  $d_K \rightarrow 0$  as  $K \rightarrow \infty$ .

For every  $K, l \in \mathbb{N}$  with  $K < l$  there exists a constant  $C_{K,l}$  such that the following hold: For every  $G \in \mathcal{G}^{(K)} \setminus \mathcal{G}_\infty^{(K)}$ , almost every  $x \in G$  and almost every  $\nu \in S^{d-1}$ , where  $S^{d-1}$  denotes the unit  $(d-1)$ -sphere, the set  $N_{G,l,x,\nu} := \Gamma_l \cap \{x + t\nu : t \in \mathbb{R}\} \cap G$  is finite with  $\#N_{G,l,x,\nu} \leq C_{K,l}$ . We write  $C_l := C_{0,l}$  and assume that for every  $K \in \mathbb{N}$  the number

$$r_K := \sup_{l > K} C_{K,l} / C_{0,l}$$

exists and  $\sup_K r_K < \infty$ .

**Example 2.1** (A Cantor-Set in 3D proposed in [21]). Consider the cube  $\mathbb{C} = [0, 1]^3$  in  $\mathbb{R}^3$  with canonical basis  $(e_i)_{i=1, \dots, 3}$  and construct  $(\Gamma_k)_{k \in \mathbb{N}}$  according to the following algorithm. Set  $\Gamma^{(0)} = \Gamma_0 = \partial\mathbb{C}$ . For  $k \in \mathbb{N} \cup \{0\}$  define

$$\tilde{\Gamma}_{k+1} := \Gamma^{(k)} \cup (e_2 + \Gamma^{(k)}) \cup (e_3 + \Gamma^{(k)}) \cup (e_3 + e_1 + \Gamma^{(k)}) \cup (e_2 + e_1 + \Gamma^{(k)}) \cup (e_3 + e_2 + e_1 + \Gamma^{(k)})$$

and

$$\Gamma_{k+1} := \left( \frac{1}{2} \tilde{\Gamma}_{k+1} \right) \setminus \Gamma_k.$$

This implies that  $\Gamma^{(K+1)} = \frac{1}{2} \tilde{\Gamma}_{K+1}$  and  $\Gamma$  is self-similar by construction. We furthermore infer  $d_K = 2^{-K}$  and  $C_k = 2^{k-1}$ . This distribution has fractal dimension  $\ln 6 / \ln 2$  which is in good agreement with experimental studies which often yield  $D \approx 2.5$  in (1) (see [21]).

## 2.2 Function spaces

In this section, we recall and adopt some notation that was originally introduced by Hummel [13] in the framework of stochastic homogenization.

**Definition 2.2** (Normal Field). Let  $e_0 = 0$  and  $(e_i)_{i=1,\dots,d}$  be the canonical basis of  $\mathbb{R}^d$ . Define:

$$D^{d-1} := \{\nu \in S^{d-1} \mid \exists m \in \{1, \dots, d\} : \nu \cdot e_i = 0 \ \forall i \in \{0, 1, \dots, m-1\} \text{ and } \nu \cdot e_m > 0\}$$

Thus, for every  $\nu \in S^{d-1}$  it holds  $\nu \in D^{d-1}$  if and only if  $-\nu \notin D^{d-1}$ .

For  $K \in \mathbb{N}$  and  $x \in \Gamma^{(K)}$ , we denote  $\nu_x \in D^{d-1}$  the normal vector to  $\Gamma^{(K)}$  in  $x$ , whenever this choice is unique (i.e. at  $C^1$ -points of  $\Gamma^{(K)}$ ). Let

$$\mathcal{C}_{K,0}^1(\mathbf{Q}) := \{u \in C(\overline{\mathbf{Q}} \setminus \Gamma^{(K)}) : \nabla u \in C(\overline{\mathbf{Q}} \setminus \Gamma^{(K)}), u|_{\partial \mathbf{Q}} \equiv 0\}$$

and for  $u \in \mathcal{C}_{K,0}^1(\mathbf{Q})$  define

$$u_{\pm}(x) := \lim_{h \rightarrow 0} (u(x \pm h\nu_x)), \quad \llbracket u \rrbracket(x) := u_+(x) - u_-(x).$$

For two points  $x, y \in \mathbb{R}^d$  denote  $(x, y)$  the closed straight line segment connecting  $x$  and  $y$ . For  $\xi \in (x, y) \cap \Gamma$  denote

$$\llbracket u \rrbracket_{x,y}(\xi) := \lim_{h \rightarrow 0} (u(\xi + h(y-x)) - u(\xi - h(y-x)))$$

the jump of the function  $u$  at  $\xi$  in direction  $(y-x)$ .

Given a function  $f \in L^2(\mathbf{Q})$  and a constant  $\mathfrak{c} > 0$ , define for  $K \in \mathbb{N}$  the following functionals on  $L^2(\mathbf{Q})$ :

$$\mathcal{E}_K(u) := \int_{\mathbf{Q} \setminus \Gamma^{(K)}} |\nabla u|^2 + \sum_{k=1}^K (1 + \mathfrak{c})^k C_k \int_{\Gamma_k} A \llbracket u \rrbracket^2 - \frac{1}{2} \int_{\mathbf{Q}} f \cdot u, \quad (2)$$

and where  $A : \Gamma \rightarrow \mathbb{R}$  with  $0 < \mathfrak{a} \leq A < \mathfrak{A} < \infty$ ,  $\mathfrak{a}, \mathfrak{A} \in \mathbb{R}$ . We introduce the scalar product

$$\langle u, v \rangle_K := \int_{\mathbf{Q}} \nabla u \cdot \nabla v + \left(1 + \frac{1}{\mathfrak{c}}\right) \sum_{k=1}^K (1 + \mathfrak{c})^k C_k \int_{\Gamma_k} \llbracket u \rrbracket \llbracket v \rrbracket$$

with the corresponding norm  $\|u\|_K^2 := \langle u, u \rangle_K$  and define  $\mathcal{H}_K := \text{closure}_{\|\cdot\|_K} \mathcal{C}_{K,0}^1(\mathbf{Q})$ . We denote  $\mathcal{H}$  the space of all measurable functions  $u$  such that there exists a family of functions  $u_K \in \mathcal{H}_K$  with  $u_K \rightarrow u$  in  $L^2(\mathbf{Q})$  and

$$\forall \varepsilon > 0 \exists K_0 \in \mathbb{N} : \forall L > K > K_0 \ \|u_K - u_L\|_L < \varepsilon. \quad (3)$$

Hence, we obtain for such a sequence that there exists  $g_u \in L^2(\mathbf{Q} \setminus \Gamma)$  and  $j_u : \Gamma \rightarrow \mathbb{R}$  such that

$$\begin{aligned} \nabla u_K &\rightarrow g_u \quad \text{strongly in } L^2(\mathbf{Q} \setminus \Gamma), \\ \forall k \in \mathbb{N} : \llbracket u_K \rrbracket &\rightarrow j_u \quad \text{strongly in } L^2(\Gamma_k). \end{aligned}$$

We write  $\nabla u := g_u$  and  $[[u]] := j_u$ . The natural scalar product on  $\mathcal{H}$  is

$$\langle u, v \rangle := \int_{Q \setminus \Gamma} \nabla u \cdot \nabla v + \left(1 + \frac{1}{\mathfrak{c}}\right) \sum_{k=1}^{\infty} (1 + \mathfrak{c})^k C_k \int_{\Gamma_k} [[u]][[v]]. \tag{4}$$

with the corresponding norm  $\|\cdot\|_{\mathcal{H}}^2 := \langle \cdot, \cdot \rangle$  and a sequence  $u_K \in \mathcal{H}_K$  converges to  $u \in \mathcal{H}$  with respect to  $\|\cdot\|_{\mathcal{H}}$  if and only if (3). It naturally follows that the following functional is well-defined on  $\mathcal{H}$ :

$$\mathcal{E}(u) := \int_{Q \setminus \Gamma} |\nabla u|^2 + \sum_{k=1}^{\infty} (1 + \mathfrak{c})^k C_k \int_{\Gamma_k} A [[u]]^2 - \frac{1}{2} \int_Q f \cdot u,$$

where we set  $\mathcal{E}(u) = +\infty$  whenever  $u \notin \mathcal{H}$ .

*Remark 2.3.* Since  $\Gamma$  might be of fractal- (and Hausdorff-) dimension bigger than  $d-1$ , in general we cannot introduce  $L^2(\Gamma; \mathcal{H}^{d-1})$  and hence we cannot write  $[[u_K]] \rightarrow j_u$  in  $L^2(\Gamma)$ , since we did not clarify, what measure to choose. However, it turns out that we do not need to know this measure for our purpose.

### 2.3 Main results

Using the above function spaces and the Poincaré inequality (8) below, we will prove the following lemma (see Section 4 for a proof).

**Lemma 2.4.** *The functionals  $\mathcal{E}$  and  $\mathcal{E}_K$  are quadratic and coercive in  $L^2(Q)$ ,  $\mathcal{H}$  and  $\mathcal{H}_K$ . Furthermore, the sequence  $\mathcal{E}_K$  Mosco-converges to  $\mathcal{E}$  in  $L^2(Q)$  (in  $\mathcal{H}$ ) as  $K \rightarrow \infty$ .*

This lemma implies uniqueness of minimizers and strong convergence of minimizers of  $\mathcal{E}_K$  to the minizer of  $\mathcal{E}$  in  $L^2(Q)$  (in  $\mathcal{H}$ ) as  $K \rightarrow \infty$ . We are particularly interested in the order of convergence of minimizers. To this aim, we will use an argument from standard a posteriori estimates in numerical analysis. However, we need some more assumptions on the geometry. We will denote these geometries as *regular* in the following.

**Definition 2.5.** A family of interfaces  $\Gamma_k$  is called regular if it satisfies the above assumptions and additionally the following two conditions

1. For every  $K \in \mathbb{N}$ ,  $\mathcal{G}^{(K)}$  consists of rectangular boxes.
2. There exists a constant  $\mathfrak{g}$  such that for every  $K$  and every  $G \in \mathcal{G}^{(K)}$  the quotient of the smallest diameter  $d_{G^-}$  largest diameter  $d_{G^+}$  of  $G$  is smaller than  $\mathfrak{g} > d_{G^-}/d_{G^+}$ .

**Theorem 2.6.** *Let the family  $\Gamma_k$  be regular. Then for the minimizers  $u_K$  of  $\mathcal{E}_K$  and every  $L > K$  it holds*

$$\|u_L - u_K\|_{\mathcal{H}}^2 \leq \tilde{C} \mathfrak{g}^{-d} (d_K^2 + \text{diam} Q (1 + \mathfrak{c}^{-1}) \mathfrak{a}^{-1}) \|f\|_{L^2(Q)} \left( \sup_{L \geq k > K} (1 + \mathfrak{c})^{-k} C_k^{-1} d_k^{-1} \right), \tag{5}$$

where  $\tilde{C}$  is the Poincaré constant such that

$$\forall v \in H^1([0, 1]^d) \quad \int_{\partial[0,1]^d} v^2 \leq \tilde{C} \int_{[0,1]^d} (|\nabla v|^2 + |v|^2). \tag{6}$$

### 3 Poincaré inequality

In what follows, given  $u \in \mathcal{C}_{K,0}^1(\mathbf{Q})$ , we write  $\widehat{\nabla}u(x) := \nabla u(x)$  if  $x \in \mathbf{Q} \setminus \Gamma^{(K)}$  and  $\widehat{\nabla}u(x) = 0$  else. Using  $ab < \frac{1}{2c}a^2 + \frac{c}{2}b^2$ , we infer for  $u \in \mathcal{C}_{K,0}^1(\mathbf{Q})$  and  $x, y \in \overline{\mathbf{Q}} \setminus \Gamma^{(K)}$  such that  $\#(x, y) \cap \Gamma^{(K)} < \infty$

$$\begin{aligned} |u(x) - u(y)|^2 &\leq \left( \sum_{k \leq K} \sum_{\xi \in (x,y) \cap \Gamma_k} \llbracket u \rrbracket_{x,y}(\xi) + \int_0^1 \widehat{\nabla}u(x + s(y-x)) \cdot (x-y) ds \right)^2 \\ &< \left(1 + \frac{1}{c}\right) |x-y|^2 \int_0^1 |\widehat{\nabla}u(x + s(y-x))|^2 ds + (1+c) \left( \sum_{k \leq K} \sum_{\xi \in (x,y) \cap \Gamma_k} \llbracket u \rrbracket_{x,y}(\xi) \right)^2 \\ &< \left(1 + \frac{1}{c}\right) |x-y|^2 \int_0^1 |\widehat{\nabla}u(x + s(y-x))|^2 ds + (1+c) \left(1 + \frac{1}{c}\right) \left( \sum_{\xi \in (x,y) \cap \Gamma_1} \llbracket u \rrbracket_{x,y}(\xi) \right)^2 \\ &\quad + (1+c)^2 \left( \sum_{k=2}^K \sum_{\xi \in (x,y) \cap \Gamma_k} \llbracket u \rrbracket_{x,y}(\xi) \right)^2. \end{aligned}$$

Since, by definition of  $C_k$ , there holds

$$\left( \sum_{\xi \in (x,y) \cap \Gamma_k} \llbracket u \rrbracket_{x,y}(\xi) \right)^2 \leq C_k \sum_{\xi \in (x,y) \cap \Gamma_k} \llbracket u \rrbracket^2(\xi)$$

we inductively obtain

$$\begin{aligned} |u(x) - u(y)|^2 &< \left(1 + \frac{1}{c}\right) |x-y|^2 \int_0^1 |\widehat{\nabla}u(x + s(y-x))|^2 ds \\ &\quad + \left(1 + \frac{1}{c}\right) \sum_{k=1}^K (1+c)^k C_k \sum_{\xi \in (x,y) \cap \Gamma_k} \llbracket u \rrbracket^2(\xi). \end{aligned} \quad (7)$$

Based on these observations, we obtain:

**Lemma 3.1** (Poincaré inequality). *The space  $\mathcal{H} = \text{dom}\mathcal{E}$  is linear and complete and for every  $s \in [0, \frac{1}{2})$  there exists a positive constant  $C_s > 0$  such that for every  $u \in \mathcal{H}$  it holds*

$$\|u\|_{H^s(\mathbf{Q})}^2 \leq (1+c^{-1}) C_s \left( \sum_{k=1}^{\infty} (1+c)^k C_k \int_{\Gamma_k} \llbracket u \rrbracket^2 + \|\nabla u\|_{L^2(\mathbf{Q} \setminus \Gamma)}^2 \right). \quad (8)$$

Furthermore, for every  $u \in \mathcal{H}$  and every  $\boldsymbol{\eta} \in \mathbb{R}^d$  it holds

$$\int_{\mathbf{Q}} |u(x) - u(x + \boldsymbol{\eta})|^2 dx \leq |\boldsymbol{\eta}| (1+c^{-1}) \left( \sum_{k=1}^{\infty} (1+c)^k C_k \int_{\Gamma_k} \llbracket u \rrbracket^2 + \|\nabla u\|_{L^2(\mathbf{Q} \setminus \Gamma)}^2 \right). \quad (9)$$

Using the last result, we see that  $\mathcal{H}$  is a Hilbert space and that  $\mathcal{E}(u) = \langle u, u \rangle_{\mathcal{H}} - \frac{1}{2} \langle f, u \rangle_{L^2(\mathbf{Q})}$  is a functional with domain  $\mathcal{H}$ .

*Proof.* Let  $K \in \mathbb{N}$  and  $u \in C(\overline{\mathbf{Q}} \setminus \Gamma^{(K)})$  with  $\nabla u \in C(\overline{\mathbf{Q}} \setminus \Gamma^{(K)})$  and  $u|_{\partial \mathbf{Q}} = 0$ . We fix  $\eta > 0$  and consider the orthonormal basis  $(e_i)_{i=1, \dots, d}$  of  $\mathbb{R}^d$ . Then we observe that

$$\begin{aligned} \int_{\mathbf{Q}} \sum_{\xi \in (x, x + \eta e_1) \cap \Gamma_k} [u]^2(\xi) \, dx &= \int_{\mathbb{R}} \left( \int_{\mathbb{R}^{d-1}} \sum_{\xi \in (x, x + \eta e_1) \cap \Gamma_k} [u]^2(\xi) \, dx_2 \dots dx_d \right) dx_1 \\ &\leq \int_{\mathbb{R}} \int_{\Gamma_k \cap ((x_1, x_1 + \eta) \times \mathbb{R}^{d-1})} [u]^2(x) \, d\sigma \, dx_1 \\ &\leq \eta \int_{\Gamma_k} [u]^2(x) \, dx, \end{aligned}$$

where we used that the surface elements are bigger than 1. Furthermore, we have

$$\eta^2 \int_0^1 |\widehat{\nabla} u(x + s\eta e_1)|^2 \, ds = \eta \int_0^\eta |\widehat{\nabla} u(x + se_1)|^2 \, ds.$$

Replacing  $e_1$  in the above calculations with any unit vector  $e$ , we obtain from integration of (7) with  $y = x + \eta e$  over  $\mathbf{Q}$  that

$$\int_{\mathbf{Q}} |u(x) - u(x + \eta)|^2 \, dx \leq |\eta| (1 + \mathfrak{c}^{-1}) \left( \sum_{k=1}^K (1 + \mathfrak{c})^k C_k \int_{\Gamma_k} [u]^2 + \|\nabla u\|_{L^2(\mathbf{Q} \setminus \Gamma)}^2 \right).$$

Deviding by  $\eta$  and integrating over  $\eta e \in \mathbb{R}^d$ , we obtain that for every  $s \in [0, \frac{1}{2})$  there exists a positive constant  $C_s > 0$  independent from  $u$  and  $K$  such that

$$\|u\|_{H^s(\mathbf{Q})}^2 \leq (1 + \mathfrak{c}^{-1}) C_s \left( \sum_{k=1}^K (1 + \mathfrak{c})^k C_k \int_{\Gamma_k} [u]^2 + \|\nabla u\|_{L^2(\mathbf{Q} \setminus \Gamma)}^2 \right). \quad (10)$$

Hence, by approximation, the last two estimates hold for all  $u \in \mathcal{H}_K$ . Let  $u_K \in \mathcal{H}_K$ ,  $K \rightarrow \infty$ , be a sequence satisfying (3). Estimate (10) yields that  $u_K$  is a Cauchy sequence in  $L^2(\mathbf{Q})$  and hence attains a limit function  $u \in L^2(\mathbf{Q})$ . Due to construction of  $\mathcal{H}$ , we identify  $u \in \mathcal{H}$ . Since the constant in (10) does not depend on  $K$ , we find that (9) and (8) hold for all  $u \in \mathcal{H}$ . Since elements of  $\mathcal{H}$  are characterized by Cauchy sequences of the form (3), we obtain that  $\mathcal{H}$  is complete.  $\square$

## 4 Proofs of Convergence properties

### 4.1 Notation and proof of Lemma 2.4

For simplicity of notation, we introduce the following scalar products on  $\mathcal{H}$  and  $\mathcal{H}_K$ :

$$\langle u, v \rangle_{\sim} := \int_{\mathbf{Q} \setminus \Gamma} \nabla u \cdot \nabla v + \sum_{k=1}^{\infty} (1 + \mathfrak{c})^k C_k \int_{\Gamma_k} A [u][v]. \quad (11)$$

$$\langle u, v \rangle_{K \sim} := \int_{\mathbf{Q} \setminus \Gamma} \nabla u \cdot \nabla v + \left(1 + \frac{1}{\mathfrak{c}}\right) \sum_{k=1}^K (1 + \mathfrak{c})^k C_k \int_{\Gamma_k} A [u][v], \quad (12)$$

with the corresponding norms  $\|\cdot\|_{\sim}$  and  $\|\cdot\|_{K \sim}$ . We obtain  $\|u\|_K \leq \mathfrak{a}^{-1} \|u\|_{K \sim}$  with  $\mathfrak{a}$  from (2) for every  $u \in \mathcal{H}_K$ . Furthermore, for every  $u \in \mathcal{H}$  and every  $K \in \mathbb{N}$ , the expression

$$\begin{aligned} \mathcal{P}_{K \sim}(u) &:= \arg \min_{v \in \mathcal{H}_K} \int_{\mathbf{Q} \setminus \Gamma} |\nabla u - \nabla v|^2 + \sum_{k=1}^K (1 + \mathfrak{c})^k C_k \int_{\Gamma_k} A ([u] - [v])^2 \\ &= \arg \min_{v \in \mathcal{H}_K} \|u - v\|_{\sim}^2 \end{aligned}$$

is well defined and  $\mathcal{P}_K$  is an orthogonal projection operator from  $\mathcal{H}$  onto  $\mathcal{H}_K$  with respect to the scalar product  $\langle \cdot, \cdot \rangle_{\sim}$ .

*Proof of Lemma 2.4.* Lower semicontinuity of  $\|\cdot\|_{\sim}$  implies that for a sequence  $u_K \in \mathcal{H}_K$  with  $\sup_K \|u_K\|_K < \infty$  and  $u_K \rightarrow u$  in  $L^2(\mathbf{Q})$  it follows

$$\mathcal{E}(u) \leq \liminf_{K \rightarrow \infty} \mathcal{E}_K(u_K).$$

Furthermore,  $\mathcal{P}_{K^\sim}(u) \rightarrow u$  strongly in  $\mathcal{H}$  and hence, using also Lemma 3.1 we have

$$\begin{aligned} \limsup_{K \rightarrow \infty} \mathcal{E}_K(\mathcal{P}_{K^\sim}(u)) &= \limsup_{K \rightarrow \infty} \left( \langle \mathcal{P}_{K^\sim}(u), \mathcal{P}_{K^\sim}(u) \rangle_{K^\sim} - \int_{\mathbf{Q}} f \mathcal{P}_{K^\sim}(u) \right) \\ &= \mathcal{E}(u). \end{aligned}$$

□

## 4.2 Proof of Theorem 2.6

Let us start with an outline of the proof. The aim is to estimate the residual  $\mathcal{R}_K(v) := \langle u_L - u_K, v \rangle_{\sim}$  as a linear functional on  $\mathcal{H}_L$  using its equivalent formulation

$$\begin{aligned} \forall v \in \mathcal{H}_L : \quad \mathcal{R}_K(v) &= \int_{\mathbf{Q}} f v - \int_{\mathbf{Q} \setminus \Gamma} \nabla u_K \cdot \nabla v - \sum_{k=1}^K (1 + \mathbf{c})^k C_k \int_{\Gamma_k} A[u_K][v] \\ &= - \sum_{k=K+1}^L \int_{\Gamma_k} \partial_\nu u_K[v], \end{aligned} \quad (13)$$

and  $\|u_L - u_K\|_{\sim}^2 = \|\mathcal{R}_K\|_{\mathcal{H}_L^*}^2$ . In order to arrive at the right hand side of (13) one needs sufficient regularity of  $\partial_\nu u_K$  and a formula of partial integration such that for every  $v \in \mathcal{H}$ ,

$$\int_{\mathbf{Q} \setminus \Gamma} \nabla u_K \cdot \nabla v + \sum_{k=1}^K (1 + \mathbf{c})^k C_k \int_{\Gamma_k} A[u_K][v] - \sum_{k=K+1}^{\infty} \int_{\Gamma_k} \partial_\nu u_K[v] = \int_{\mathbf{Q}} f v. \quad (14)$$

Thus, in Step 1, we will prove the regularity of  $\partial_\nu u_K$  and provide an a priori estimate on  $\partial_\nu u_K$  that is sufficient to derive (5) from (13). For this we will use standard method that can be found in [7]. In Step 2, we will prove (14) and in Step 3 we will combine the a priori estimate from Step 1 with (13) in order to conclude the proof.

### Step 1: Higher regularity for $\partial_i u$ on special subsets.

For  $h \in \mathbb{R}^d$ ,  $i \in (1, \dots, d)$  and  $u \in H^1(\mathbb{R}^d)$  we write

$$D_i^h u(x) := \frac{1}{h} (u(x + h e_i) - u(x))$$

and for a smooth function with compact support  $\varphi \in C_c^\infty(\mathbb{R}^d)$  we recall that

$$\begin{aligned} \int_{\mathbb{R}^d} |D_i^h u|^2 &\leq \int_{\mathbb{R}^d} \frac{1}{h^2} \left| \int_0^h \partial_i u(x + t e_i) dt \right|^2 dx \leq \int_{\mathbb{R}^d} \frac{1}{h^2} h \int_0^h |\partial_i u(x + t e_i)|^2 dt dx \\ &\leq \frac{1}{h} \int_0^h \int_{\mathbb{R}^d} |\partial_i u(x + t e_i)|^2 dx dt \\ &= \int_{\mathbb{R}^d} |\partial_i u|^2 \end{aligned} \quad (15)$$

Let  $K \in \mathbb{N}$  and  $G \in \mathcal{G}^{(K)} \setminus \mathcal{G}_\infty^{(K)}$ . For simplicity of notation, we assume that  $G = (-g, g)^d$ .

Let  $L > K$ . Let  $\xi_L \in C_c^\infty(\mathbb{R})$  be such that  $\xi_L(t) = 1$  if  $|t| < g - d_L$  and  $\xi_L(t) = 0$  if  $|t| > g$  and with  $|\xi'_L| \leq 2d_L^{-1}$ . Furthermore, let  $\xi_G \in C_c^\infty(\mathbb{R}^d)$  be point-symmetric in 0 with  $\xi_G|_G \equiv 1$ ,  $\xi_G \geq 0$  and  $|\nabla \xi_G| < 2g^{-1}$  and write  $\tilde{\xi}_{L,i}(x) := \xi_L(x_i)\xi_G(x)$ . For  $h \in \mathbb{R}_{>0}$ , we define  $v_h(x) := -D_i^{-h}(\tilde{\xi}_{L,i}^2 D_i^h u_K(x))$  with  $v_h \in \mathcal{H}_K$  and obtain

$$\int_{\mathcal{Q}} \nabla u_K \cdot \nabla v_h + \sum_{k=1}^K (1 + \mathfrak{c})^{-k} C_k^{-1} \int_{\Gamma_k} \llbracket u_K \rrbracket \llbracket v_h \rrbracket = \int_{\mathcal{Q}} f v_h,$$

which implies by (15)

$$\begin{aligned} \int_{\mathcal{Q}} \tilde{\xi}_{L,i}^2 |\nabla D_i^h u_K|^2 + \sum_{k=1}^K (1 + \mathfrak{c})^{-k} C_k^{-1} \int_{\Gamma_k} \tilde{\xi}_{L,i}^2 \llbracket D_i^h u_K \rrbracket \llbracket D_i^h u_K \rrbracket \\ \leq \|f\|_{L^2(2G)} \|D_i^{-h}(\tilde{\xi}_{L,i}^2 D_i^h u_K)\| + 4d_L^{-1} \int_{\mathcal{Q}} \tilde{\xi}_{L,i} |\nabla D_i^h u_K| |D_i^h u_K| \\ \leq \|f\|_{L^2(2G)} \|\partial_i(\tilde{\xi}_{L,i}^2 D_i^h u_K)\| + 4d_L^{-1} \int_{\mathcal{Q}} \tilde{\xi}_{L,i} |\nabla D_i^h u_K| |D_i^h u_K| \\ \leq \|f\|_{L^2(2G)} \left( \|\tilde{\xi}_{L,i}^2 \partial_i D_i^h u_K\|_{L^2(\mathcal{Q})} + 2d_L^{-1} \|\tilde{\xi}_{L,i} D_i^h u_K\|_{L^2(\mathcal{Q})} \right) \\ + 2 \left( \frac{1}{4} \|\tilde{\xi}_{L,i} \nabla D_i^h u_K\|_{L^2(\mathcal{Q})}^2 + 4d_L^{-2} \|D_i^h u_K\|_{L^2(2G)}^2 \right) \end{aligned}$$

Hence, we obtain

$$\frac{1}{4} \int_{\mathcal{Q}} \tilde{\xi}_{L,i}^2 |\nabla D_i^h u_K|^2 \leq 4 \|f\|_{L^2(\mathcal{Q})}^2 + d_L^{-2} \|\tilde{\xi}_{L,i} D_i^h u_K\|_{L^2(\mathcal{Q})}^2 + 8d_L^{-2} \|D_i^h u_K\|_{L^2(\mathcal{Q})}^2.$$

Denoting  $G_{\xi,L,i} := \{x \in G : \tilde{\xi}_{L,i}(x_i) = 1\}$  we hence find with help of (15)

$$\int_{G_{\xi,L,i}} |\nabla \partial_i u_K|^2 \leq 36 \left( \|f\|_{L^2(2G)}^2 + d_L^{-2} \|\partial_i u_K\|_{L^2(2G)}^2 \right). \quad (16)$$

Moreover, we find for every interface

$$\Upsilon := \{x \in \Gamma_L \cap G : e_i \text{ is normal in } x\}$$

with help of (6) and (16) that

$$\begin{aligned} d_L \|\partial_i u_K\|_{L^2(\Upsilon)}^2 &\leq \mathfrak{g}^{-d} \tilde{C} \left( d_L^2 \|\nabla \partial_i u_K\|_{L^2(G_{\xi,L,i})}^2 + \|\partial_i u_K\|_{L^2(G)}^2 \right) \\ &\leq \mathfrak{g}^{-d} \tilde{C} \left( d_L^2 \|f\|_{L^2(2G)}^2 + \|\partial_i u_K\|_{L^2(2G)}^2 + \|\partial_i u_K\|_{L^2(G)}^2 \right). \end{aligned} \quad (17)$$

**Step 2: Proof of the identity (14).**

For a measurable set  $A \subset \mathbb{R}^d$ , let

$$d_{A,G}^\varepsilon(x) := \begin{cases} \max \left\{ 1 - \frac{1}{\varepsilon} \inf_{y \in A} |x - y|, 0 \right\} & \text{if } x \in G \\ 0 & \text{else} \end{cases}.$$

Moreover, we define  $\Gamma^{(K,L)} := \bigcup_{k=K+1}^L \Gamma_k$  and the function

$$d^\varepsilon(x) := \sum_{G \in \mathcal{G}_K} d_{\Gamma^{(K,L)},G}^\varepsilon(x).$$

Then, for every  $v \in \mathcal{C}_{L,0}^1(\mathbf{Q})$ , we have  $v(1 - d^\varepsilon) \in \mathcal{H}_K$  and

$$\int_{\mathbf{Q} \setminus \Gamma} \nabla u_K \cdot \nabla (v(1 - d^\varepsilon)) + \sum_{k=1}^K (1 + \mathbf{c})^k C_k \int_{\Gamma_k} A[u_K][v(1 - d^\varepsilon)] = \int_{\mathbf{Q}} f v(1 - d^\varepsilon). \quad (18)$$

Moreover, we have

$$\sum_{k=1}^K (1 + \mathbf{c})^k C_k \int_{\Gamma_k} A[u_K][v d^\varepsilon] \rightarrow 0 \quad \text{as } \varepsilon \rightarrow 0 \quad (19)$$

and

$$\int_{\mathbf{Q} \setminus \Gamma} \nabla u_K \cdot \nabla (v d^\varepsilon) = \int_{\mathbf{Q} \setminus \Gamma} d^\varepsilon \nabla u_K \cdot \nabla v + \int_{\mathbf{Q} \setminus \Gamma} v \nabla u_K \cdot \nabla d^\varepsilon. \quad (20)$$

Since  $\partial_\nu u$  is locally in  $H^1$  close to each  $\Gamma_k$ ,  $k > K$ , we find in the limit that

$$\int_{\mathbf{Q} \setminus \Gamma} v \nabla u_K \cdot \nabla d^\varepsilon \rightarrow - \sum_{k=K+1}^L \int_{\Gamma_k} \partial_\nu u_K[v] \quad \text{as } \varepsilon \rightarrow 0. \quad (21)$$

We then find (14) from summing up (18) and (20) and using the limit behavior (19) and (21).

### Step 3: The residual.

From the Poincaré inequality (9) we obtain that minimizers  $u_K$  of  $\mathcal{E}_K$  satisfy

$$\|u_K\|_{\mathcal{H}} \leq \text{diam} \mathbf{Q} (1 + \mathbf{c}^{-1}) \mathbf{a}^{-1} \|f\|_{L^2(\mathbf{Q})}.$$

Starting from (13) we estimate the residual through

$$\begin{aligned} |\mathcal{R}_K(v)|^2 &\leq \left| \sum_{k=K+1}^L \int_{\Gamma_k} \left( (1 + \mathbf{c})^{-\frac{k}{2}} C_k^{-\frac{1}{2}} \partial_\nu u_K \right) \left( (1 + \mathbf{c})^{\frac{k}{2}} C_k^{\frac{1}{2}} [v] \right) \right|^2 \\ &\leq \left( \sum_{k=K+1}^L (1 + \mathbf{c})^{-k} C_k^{-1} \int_{\Gamma_k} (\partial_\nu u_K)^2 \right) \|v\|_{\mathcal{H}}^2 \end{aligned}$$

and we find with help of  $\|u_L - u_K\|_{\sim}^2 = \|\mathcal{R}_K\|_{\mathcal{H}^*}^2$  and (17) that

$$\begin{aligned} \|u - u_K\|_{\sim}^2 &= \|\mathcal{R}_K\|_{\mathcal{H}^*}^2 \leq \sum_{k=K+1}^L (1 + \mathbf{c})^{-k} C_k^{-1} d_k^{-1} d_k \int_{\Gamma_k} (\partial_\nu u_K)^2 \\ &\leq \sum_{k=K+1}^L \sum_{G \in \mathcal{G}_\infty^{(k)} \setminus \mathcal{G}_\infty^{(k-1)}} (1 + \mathbf{c})^{-k} C_k^{-1} d_k^{-1} \mathbf{g}^{-d} \tilde{C} (d_K^2 \|f\|_{L^2(2G)}^2 + 2 \|\partial_i u_K\|_{L^2(2G)}^2) \\ &\leq \mathbf{g}^{-d} \tilde{C} (d_K^2 + \text{diam} \mathbf{Q} (1 + \mathbf{c}^{-1}) \mathbf{a}^{-1}) \|f\|_{L^2(\mathbf{Q})} \left( \sup_{L \geq k > K} (1 + \mathbf{c})^{-k} C_k^{-1} d_k^{-1} \right). \end{aligned}$$

## 5 Iterative numerical homogenization

This section is limited to a description of the proposed numerical method. We will comment on the strategy for a convergence proof, but the details will be shifted to an upcoming publication with an emphasis on numerical analysis.

Denote with  $\mathcal{T}_0$  an initial, shape regular partition of  $\mathbf{Q}$  into simplices with maximal diameter  $h_0 > 0$  that resolves the level interface network  $\Gamma^{(0)}$ . Similarly, each member of the sequence  $(\mathcal{T}_K)_{K \in \mathbb{N}}$  is a regular partition of  $\mathbf{Q}$  into simplices with maximal diameter  $h_K > 0$  obtained by conforming refinement of  $\mathcal{T}_{K-1}$ , that resolves the level interface network  $\Gamma^{(K)}$ .

With the associated piecewise linear Lagrange or nodal basis functions  $\lambda_x^{(K)}$ ,  $x \in \mathcal{N}_K$ , where  $\mathcal{N}_K \subset \mathbf{Q}$  is the set of interior vertices of  $\mathcal{T}_K$ , we define local, piecewise affine finite element spaces

$$S_i^{(K)} = \text{span}\{\lambda_x^{(K)}|_{G_i^{(K)}} : x \in \mathcal{N}_K \cap \overline{G_i^{(K)}}\} \subset H^1(G_i^{(K)}), \quad S^{(K)} = \bigoplus_{i=1}^{I_K} S_i^{(K)} \subset \mathcal{H}$$

for each cell  $G_i^{(K)}$  on level  $K$  and a corresponding global, piecewise affine finite element space that allows for discontinuities across  $\Gamma^{(K)}$ .

To each vertex  $x \in \mathcal{N}_K$ , we assign a local patch  $\omega_x^{(K+1)} \subset \overline{\mathbf{Q}}$  given by the support of the respective nodal basis function consisting of the union of elements in  $\mathcal{T}_K$  containing  $x$ . More precisely, define the following hierarchy of patches

$$\begin{aligned} \mathbf{Q}^{(0)} &= \{\overline{\mathbf{Q}}\} \\ \mathbf{Q}^{(1)} &= \{\omega_x^{(1)} \subset \overline{\mathbf{Q}} : \omega_x^{(1)} = \text{supp } \lambda_x^{(0)}, \quad x \in \mathcal{N}_0\} \\ \mathbf{Q}^{(K)} &= \{\omega_x^{(K)} \subset \overline{\mathbf{Q}} : \omega_x^{(K)} = \text{supp } \lambda_x^{(K-1)}, \quad x \in \mathcal{N}_{K-1}\} \end{aligned}$$

and denote with  $\mathcal{H}(\omega) := \{v|_{\text{interior}(\omega)} : v \in \mathcal{H}, v|_{\partial\omega} \equiv 0\} \subset \mathcal{H}$  the restrictions of  $v \in \mathcal{H}$  to  $\omega \in \mathbf{Q}^{(K)}$  with zero Dirichlet boundary condition. Furthermore, the local finite element spaces associated to each patch  $\omega \in \mathbf{Q}^{(K)}$  read

$$S_\omega = S^{(K)} \cap \mathcal{H}(\omega).$$

We refrain from stating the dependence of  $S_\omega$  and  $\mathcal{H}(\omega)$  on  $K$  explicitly, but rely on the individual context,  $\omega \in \mathbf{Q}^{(K)}$ , to provide the information. The functions in the finite element spaces allow for discontinuities across the edges that resolve the interface network  $\Gamma^{(K)}$  but are otherwise continuous. They will serve to represent a hierarchy of frequencies of functions in the solution space. The coarsest space  $S_{\overline{\mathbf{Q}}}$  establishes a global transport of information in the iterative process.

We consider the multilevel splitting

$$\mathcal{H} = \sum_{k=0}^{K-1} \sum_{\omega \in \mathbf{Q}^{(k)}} S_\omega + \sum_{\omega \in \mathbf{Q}^{(K)}} \mathcal{H}(\omega)$$

which provides the preconditioner

$$T_K = \sum_{k=0}^{K-1} \sum_{\omega \in \mathbf{Q}^{(k)}} P_{S_\omega} + \sum_{\omega \in \mathbf{Q}^{(K)}} P_{\mathcal{H}(\omega)} \quad (22)$$

and induces an additive Schwarz method. Here, the operators  $P_V : \mathcal{H} \rightarrow V$  denote orthogonal projections from the solution space  $\mathcal{H}$  to its subspaces  $V$  in the sense of the inner product (4), defined via the equation

$$\langle P_V w, v \rangle = \langle w, v \rangle, \quad \forall v \in V. \quad (23)$$

After fixing a starting value  $u^{(0)} = w^{(0)}$ , the solution  $u$  of the boundary value problem is approximated by a CG method

$$u^{(\nu)} = \sum_{l=0}^{\nu} \alpha_{\nu l} w^{(l)}, \quad \sum_{l=0}^{\nu} \alpha_{\nu l} = 1,$$

whose iterates  $u^{(\nu)}$  consist of weighted averages of the basic iterates

$$w^{(l+1)} = w^{(l)} + T_K(u - w^{(l)}).$$

However, the preconditioner (22) is computationally unfeasible, since evaluating the local projections  $P_{\mathcal{H}(\omega)}$ ,  $\omega \in \mathbf{Q}^{(K)}$ , amounts to solving continuous variational problems. Therefore, we replace the continuous spaces  $\mathcal{H}(\omega)$ ,  $\omega \in \mathbf{Q}^{(K)}$ , with finite element spaces  $S_\omega \subset \mathcal{H}(\omega)$  and consider the discrete splitting

$$S^{(K)} = \sum_{k=0}^K \sum_{\omega \in \mathbf{Q}^{(k)}} S_\omega$$

with associated preconditioner

$$\tilde{T}_K = \sum_{k=0}^K \sum_{\omega \in \mathbf{Q}^{(k)}} P_{S_\omega}. \quad (24)$$

As a consequence, all level interface networks after level  $K$  and hence all contributions from finer interfaces are truncated. Note that Theorem 2.6 tells us that the resulting modeling error is small. Once per CG step, the preconditioner  $\tilde{T}_K$  is evaluated by computing the Ritz projections (23) to all  $S_\omega$ ,  $\omega \in \mathbf{Q}^{(k)}$ ,  $k \leq K$ . As the local bases of these subspaces are restricted nodal basis functions, this comes down to solving a symmetric, positive-definite, linear system per patch. This preconditioner can be interpreted as a generalized Jacobi smoother, whose blocks are defined by the hierarchy of patches.

*Remark 5.1.* Since the introduced scheme is an instance of an additive Schwarz method, it is natural to rely on the established subspace correction framework [22, 23] to prove convergence and conduct further analysis. An extension to the case with an infinite dimensional solution space was presented in [17]. The key is to show the stability of the multilevel splitting. Then, basic results imply spectral equivalence and an application of the spectral mapping theorem yields the usual error bounds for preconditioned CG iterations in function space. Choosing the averaging coefficients  $\alpha_{\nu l}$  according to the CG method guarantees a minimal energy error  $\|u - u^{(\nu)}\|_{\mathcal{H}}$  and thus optimal convergence rates.

## 5.1 Numerical experiments

In this exposition, we consider numerical examples in two dimensions with the Cantor set presented in Example 2.1 as well as an interface geometry reminding one of geological fault networks. For this purpose, the unit square  $\mathbf{Q} = (0, 1)^2 \subset \mathbb{R}^2$  is partitioned uniformly into squares of edge length  $h_J = 2^{-J}$  and the simplicial partitions  $\mathcal{T}_J$  are obtained by further subdividing each square into two triangles. Any of these triangulations  $\mathcal{T}_J$  with  $h_J \leq 2^{-K}$  is able to resolve the Cantor level interface network  $\Gamma^{(K)}$ .

We consider the variational formulation associated with the energy (2)

$$\text{find } \tilde{u}_K \in S^{(K)} : \quad \langle \tilde{u}_K, v \rangle_K = \int_{Q \setminus \Gamma^{(K)}} f \cdot v, \quad \forall v \in S^{(K)} \quad (25)$$

with zero Dirichlet boundary conditions,  $A \equiv 1$ ,  $f \equiv 1$  and parameters  $\mathbf{c} = 1$  as well as  $C_K = 2^{K-1}$  given by the geometry of the Cantor interface network.

### 5.1.1 Convergence test with direct solver

Notice that the Cantor set from Example 2.1 satisfies the regularity assumptions of Definition 2.5 thus enabling the application of Theorem 2.6. Since the considered interface network has tensor structure and  $1/(C_K d_K) = 2$ , we expect an exponential convergence with analytic bound

$$\|u - u_K\|_{\mathcal{H}}^2 \leq c(1 + \mathbf{c})^{-K},$$

where  $c$  is a constant that is independent of  $K$ . Note that the analytical estimate may not be optimal. To assess the quality of this convergence estimate numerically, we assemble the discrete variational problem (25) for one triangulation  $\mathcal{T}_9$  with different level interface networks  $\Gamma^{(K)}$  (see e.g. Figure 3),  $K = 1, \dots, 9$ , solve the resulting linear systems directly and denote the finite element solutions with  $\tilde{u}_K$ . The remaining discretization error is estimated by  $\|\tilde{u}_{10} - \tilde{u}_9\|_{\mathcal{H}}$ , where  $\tilde{u}_{10}$  denotes the solution of (25) with  $\Gamma^{(10)}$  on  $\mathcal{T}_{10}$ . The numerical estimates

$$\|u - u_K\|_{\mathcal{H}} \leq \|u - u_9\|_{\mathcal{H}} + \|u_9 - u_K\|_{\mathcal{H}} \approx \|\tilde{u}_{10} - \tilde{u}_9\|_{\mathcal{H}} + \|\tilde{u}_9 - \tilde{u}_K\|_{\mathcal{H}}$$

for  $K = 1, \dots, 8$  are recorded in Figure 2. As illustrated, the numerical experiment confirms the analytic convergence result.

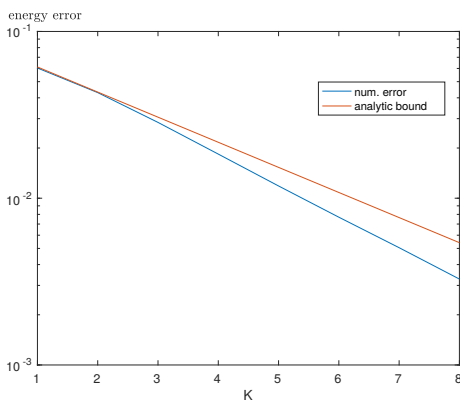


Figure 2: Convergence test

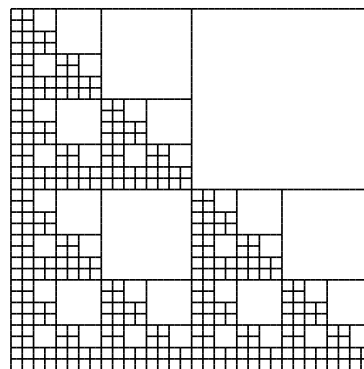


Figure 3: Cantor set  $\Gamma^{(5)}$

### 5.1.2 Iterative numerical homogenization of Cantor interfaces

Again,  $\tilde{u}_K$  denotes the exact finite element solution of the discrete variational problem (25) with level interface network  $\Gamma^{(K)}$  and triangulation  $\mathcal{T}_K$ . Correspondingly,  $\tilde{u}_K^{(\nu)}$  are the iterates of the preconditioned CG iteration with preconditioner  $\tilde{T}_K$  given in (24) and initial iterate  $\tilde{u}_K^{(0)} = \tilde{u}_0$  for the same problem. The factors by which the energy norm of the

Table 1: Reduction factors of the numerical method for Cantor interfaces

$\nu$	$K = 5$	$K = 6$	$K = 7$	$K = 8$	$K = 9$
1	0.479	0.481	0.481	0.482	0.482
2	0.445	0.464	0.483	0.500	0.514
3	0.453	0.448	0.442	0.437	0.439
4	0.429	0.452	0.474	0.493	0.503
5	0.451	0.465	0.468	0.472	0.477
6	0.432	0.444	0.459	0.477	0.494
7	0.447	0.467	0.463	0.456	0.455
8	0.450	0.483	0.487	0.489	0.490
$\rho_{\text{exp}}$	0.448	0.463	0.469	0.475	0.481
$\nu_{\text{stop}}$	4	5	5	6	7

error  $\|\tilde{u}_K - \tilde{u}_K^{(\nu)}\|_{\mathcal{H}}$  is reduced relative to the one for the previous iterate are presented in Table 1. The experimental convergence rates  $\rho_{\text{exp}}$  are determined by the geometric mean of the recorded reduction factors.

The computational efficiency of the method is governed by the number of iteration steps required to reduce the error below the discretization error on the finest grid. It is indicative for how fast the iterative method converges in practice and for its robustness with respect to the number of cells. Since  $\tilde{u}_{K+1} - \tilde{u}_K$  is the  $\langle \cdot, \cdot \rangle$ -orthogonal projection of  $u_K - \tilde{u}_K$  to the finite element space assigned to the grid  $\mathcal{T}_{K+1}$ , it holds  $\|\tilde{u}_{K+1} - \tilde{u}_K\|_{\mathcal{H}} \leq \|u_K - \tilde{u}_K\|_{\mathcal{H}}$ . Consequently, the aforementioned accuracy is reached as soon as the stopping criterion

$$\|\tilde{u}_K - \tilde{u}_K^{(\nu_{\text{stop}})}\|_{\mathcal{H}} \leq \|\tilde{u}_{K+1} - \tilde{u}_K\|_{\mathcal{H}} \leq \|u_K - \tilde{u}_K\|_{\mathcal{H}}$$

is satisfied after  $\nu_{\text{stop}}$  iterations. Evidently, the numerical method is very robust with respect to the grid size and the number of cells.

### 5.1.3 Iterative numerical homogenization of geological interfaces

Next, we consider the triangulations  $\mathcal{T}_K$  that are obtained by partitioning the domain uniformly into squares of edge length  $h_K = 2^{-(K+4)}$  and further subdividing each square into two triangles. Moreover, we use the same problem parameters as previously, but with different interface geometry. For this purpose, we generate a sequence of level interface networks  $\Gamma^{(K)}$  that have the superficial appearance of geological faults (see Figure 4) and does not self-intersect. The level interface network  $\Gamma^{(K)}$  is constructed by appending sequences of edges that connect boundary to boundary in the triangulation  $\mathcal{T}_K$  to the previous level interface network  $\Gamma^{(K-1)}$ . One such sequence of connected edges is supposed to resemble a geological fault (see Figure 4). In contrast to the previous setting, the number of new geological interfaces and thus the number of new cells per level  $\#(\mathcal{G}^{(K+1)} \setminus \mathcal{G}^{(K)})$  is bounded by a constant.

The reduction factors, experimentally determined convergence rates  $\rho_{\text{exp}}$  and number of iterations until the discretization accuracy is reached  $\nu_{\text{stop}}$  are collected in Table 2. Again, the numerical method displays a robust behavior with respect to the grid size and the number of cells. The lower complexity of this interface geometry, in the sense of significantly fewer new cells per level, is reflected by the method needing fewer iterations to reach the discretization accuracy.

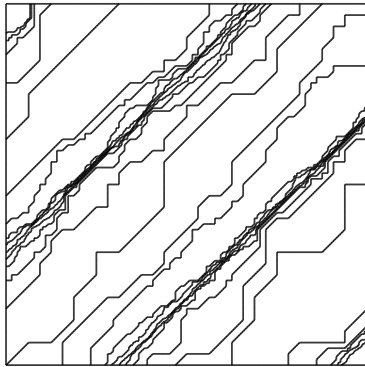


Figure 4: Geological interface geometry

Table 2: Reduction factors of the numerical method for geological interfaces

$\nu$	$K = 5$	$K = 6$	$K = 7$	$K = 8$	$K = 9$
1	0.300	0.370	0.371	0.390	0.421
2	0.200	0.439	0.478	0.500	0.521
3	0.336	0.345	0.428	0.497	0.538
4	0.376	0.393	0.420	0.492	0.516
5	0.251	0.416	0.501	0.502	0.515
6	0.325	0.410	0.422	0.494	0.518
7	0.367	0.361	0.462	0.479	0.533
8	0.324	0.450	0.421	0.496	0.520
$\rho_{\text{exp}}$	0.304	0.396	0.436	0.480	0.509
$\nu_{\text{stop}}$	1	1	1	1	1

## References

- [1] Grégoire Allaire. Homogenization and two-scale convergence. *SIAM Journal on Mathematical Analysis*, 23(6):1482–1518, 1992.
- [2] Grégoire Allaire and Marc Briane. Multiscale convergence and reiterated homogenization. *Proceedings of the Royal Society of Edinburgh Section A: Mathematics*, 126(2):297–342, 1996.
- [3] Scott Armstrong, Tuomo Kuusi, and Jean-Christophe Mourrat. Quantitative stochastic homogenization and large-scale regularity. *arXiv preprint arXiv:1705.05300*, 2017.
- [4] Scott N Armstrong and Charles K Smart. Quantitative stochastic homogenization of elliptic equations in nondivergence form. *Archive for Rational Mechanics and Analysis*, 214(3):867–911, 2014.
- [5] Doina Cioranescu, Alain Damlamian, Patrizia Donato, Georges Griso, and Rachad Zaki. The periodic unfolding method in domains with holes. *SIAM Journal on Mathematical Analysis*, 44(2):718–760, 2012.
- [6] Yalchin Efendiev and Thomas Y Hou. *Multiscale finite element methods: theory and applications*, volume 4. Springer Science & Business Media, 2009.
- [7] L.C. Evans. *Partial Differential Equations*. AMS, 1998.
- [8] Antoine Gloria, Stefan Neukamm, and Felix Otto. An optimal quantitative two-scale expansion in stochastic homogenization of discrete elliptic equations. *ESAIM: Mathematical Modelling and Numerical Analysis*, 48(2):325–346, 2014.
- [9] Georges Griso. Error estimate and unfolding for periodic homogenization. *Asymptotic Analysis*, 40(3, 4):269–286, 2004.
- [10] Martin Heida. An extension of the stochastic two-scale convergence method and application. *Asymptotic Analysis*, 72(1-2):1–30, 2011.
- [11] Ulrich Hornung. *Homogenization and porous media*, volume 6. Springer Science & Business Media, 2012.

- [12] Hans-Karl Hummel. Homogenization for heat transfer in polycrystals with interfacial resistances. *Appl. Anal.*, 75(3-4):403–424, 2000.
- [13] H.K. Hummel. *Homogenization of Periodic and Random Multidimensional Microstructures*. PhD thesis, Technische Universität Bergakademie Freiberg, 1999.
- [14] V. V. Jikov, S. M. Kozlov, and O. A. Oleĭnik. *Homogenization of differential operators and integral functionals*. Springer-Verlag, Berlin, 1994. Translated from the Russian by G. A. Yosifian [G. A. Iosif'yan].
- [15] Ralf Kornhuber, Daniel Peterseim, and Harry Yserentant. An analysis of a class of variational multiscale methods based on subspace decomposition. *Math. Comp.*, 2016. In press.
- [16] Ralf Kornhuber, Joscha Podlesny, and Harry Yserentant. Direct and iterative methods for numerical homogenization. In Chang-Ock Lee, Xiao-Chuan Cai, David E. Keyes, Hyea Hyun Kim, Axel Klawonn, Eun-Jae Park, and Olof B. Widlund, editors, *Domain Decomposition Methods in Science and Engineering XXIII*, pages 217–225. Springer International Publishing, 2017.
- [17] Ralf Kornhuber and Harry Yserentant. Numerical homogenization of elliptic multiscale problems by subspace decomposition. *Multiscale Modeling & Simulation*, 14(3):1017–1036, 2016.
- [18] Axel Målqvist and Daniel Peterseim. Localization of elliptic multiscale problems. *Mathematics of Computation*, 83(290):2583–2603, 2014.
- [19] Hiroyuki Nagahama and Kyoko Yoshii. Scaling laws of fragmentation. In *Fractals and Dynamic Systems in Geoscience*, pages 25–36. Springer, 1994.
- [20] Charles G Sammis, Robert H Osborne, J Lawford Anderson, Mavonwe Banerdt, and Patricia White. Self-similar cataclasis in the formation of fault gouge. *Pure and Applied Geophysics*, 124(1):53–78, 1986.
- [21] Donald L Turcotte. Crustal deformation and fractals, a review. In *Fractals and Dynamic Systems in Geoscience*, pages 7–23. Springer, 1994.
- [22] Jinchao Xu. Iterative methods by space decomposition and subspace correction. *SIAM Review*, 34(4):581–613, 1992.
- [23] Harry Yserentant. Old and new convergence proofs for multigrid methods. *Acta Numerica*, 2:285–326, 1993.
- [24] V. V. Zhikov and A. L. Pyatnitskiĭ. Homogenization of random singular structures and random measures. *Izv. Ross. Akad. Nauk Ser. Mat.*, 70(1):23–74, 2006.